Gear Fault Diagnosis Using Electrical Signals and its Application to Wind Power Systems

Ranjith Kumar, Michael H.Azarian, Michael G.Pecht
Center for Advanced Life Cycle Engineering
University of Maryland, College Park
Maryland, USA
ranjith@calce.umd.edu, mazarian@calce.umd.edu,
pecht@calce.umd.edu

Nam H. Kim
Department of Mechanical and Aerospace Engineering
University of Florida, Gainesville
Florida, USA
nkim@ufl.edu

***Abstract*—The objective of this paper is to investigate the detection of damage in electromechanical equipment using the electrical output signals. This can help designers in eliminating sensor redundancy as well as being a non-invasive method and a remote monitoring approach. As an example, a coupled gearbox and generator model of a wind turbine system is created. A crack in a gear tooth is introduced and modeled as a reduction in gear tooth stiffness during the meshing of the gears. The simulation results show that the angular acceleration at the side bands of mesh frequency increases according to damage severity, which is as expected. However, the frequency spectrum of electrical torque shows distinct peaks due to the gear tooth crack. It is also shown that cracks in different gears can be detected at distinct frequencies, which shows the possibility of identifying the source of cracks, providing an opportunity for diagnostics.**

Keywords-gear; crack; mesh stiffness; simulation; wind turbine; electrical torque; dynamic model

I. INTRODUCTION

Health monitoring of complex engineering systems requires the installation of expensive hardware with multiple sensors for monitoring the different components of the system. Fault detection in an electromechanical system, in which mechanical components drive or are driven by an electrical system, such as a wind turbine, can be carried out by analyzing the electrical signals of the system. Motor current signature analysis is one of the approaches in the literature which has been used to study broken rotor bars, bearing failure or winding faults in electrical motors [1]. This approach has been described in various studies in the literature for wind turbines. Yang et al. [2] used the generator output power as well as the rotational speed on a test rig for the detection of mechanical unbalance in the generator. Time-frequency analysis of the power output of the generator was used by Watson et al. [3] in the detection of the shaft misalignment in the generator. Their approach could predict the bearing failure due to shaft misalignment in the generator before the actual occurrence of bearing failure. A similar study was carried out by Crabtree et al. [4] where suggestions were given on the identification of different frequency bands in the current spectrum which would represent the different fault conditions of the mechanical components in the generator.

The approach used in this study is the detection of faults in mechanical equipment which influence or are influenced by the operation of the electrical equipment rather than those in the electrical equipment as has been carried out in the literature. Hence the objective of this paper is the detection of faults in upstream mechanical equipment using the signals of the electrical equipment that influence them. A wind turbine is considered as a case study in this paper to analyze the possibility of detection of a gear tooth crack in the gearbox using the generator electrical signals. A simulation is carried out of the operation of the gearbox and the generator of the wind turbine under faulty conditions. This is performed using a coupled dynamic model of the gearbox and generator model developed using a lumped parameter model and the direct-quadrature (d-q) framework, respectively. Electrical torque signals are used in this study for fault detection since the faults in mechanical equipment would manifest themselves in the angular velocity signal which is the input to the generator. Any changes in the angular velocity signal should be detected in the electrical torque signal of the generator. Measurement of the electrical torque can be carried out in a real application by direct or indirect methods. The indirect method is through the measurement of the current or the flux generated in the generator and mathematical manipulation for the estimation of the electrical torque. One of the direct methods is through the use of piezoelectric sensors such as that explained by Healey et al. [5] in their study.

II. DYNAMIC MODELING OF A WIND TURBINE

A dynamic model is an approximation of the actual system which retains all the essential dynamic characteristics of the system. The three basic elements used in dynamic modeling are the spring, mass, damper and a corresponding set for torsional elements. Modeling can be carried out by lumped-parameter or distributed-parameter systems. Lumped-parameter systems consider that the components are discrete, with masses assumed to be rigid and concentrated at individual points in the system. In this study, the various components of the wind turbine such as the shafts, gearbox and the generator will be considered as lumped parameter systems with equations of motion described by ordinary differential equations. Dynamic modeling has been carried out in wind turbines for studying grid disturbances and establishing control strategies for obtaining a higher power efficiency coefficient under various operating conditions of the wind turbine [6–10]. It is also used for the analysis of the various loads acting on the internal components of a wind

turbine, and for studying the stability of the structure under different wind conditions [11], [12]. A dynamic model based on the d-q reference frame is used in this analysis in order to model fast transients in both the stator and rotor flux of the DFIG.

A. *Dynamic modeling of the gearbox*

The model of the gearbox considered in this study is a three stage gearbox based on [11]. It consists of a sun-and-planet gear stage which receives the input torque from the wind, followed by two parallel gear stages. The total gear ratio of this gearbox is 34.7. A schematic of the sun and planet stage of the gearbox is shown in Fig. 1.

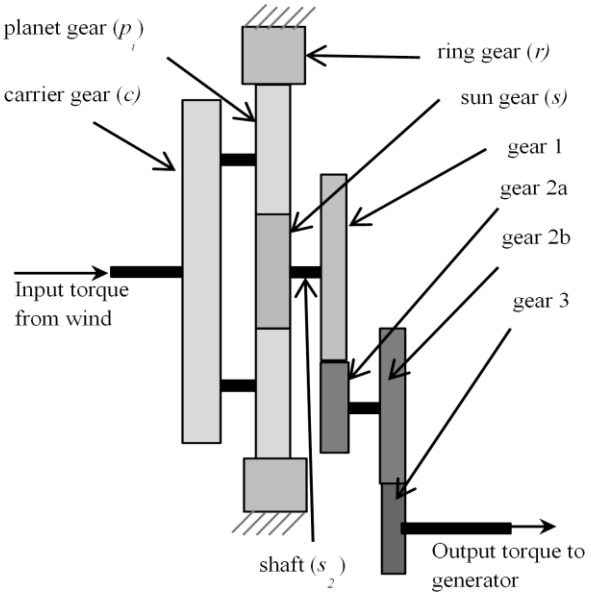

Figure 1. Schematic of gearbox layout

Input torque from the wind is transmitted to the carrier gear, which is the input gear for the gearbox. The output gear of the gearbox is labeled as gear 3 in the figure, which transmits the torque to the generator. Mechanical coupling between gear stages is modeled using a spring-dashpot system to represent the gear tooth interactions. The friction in contact surfaces between gear teeth is not considered in this model. The stiffness of the spring is modeled as a time-varying rectangular function corresponding to the single pair tooth contact and double pair tooth contact [13]. The variation of tooth bending stiffness considered in this study is shown in Fig. 2.

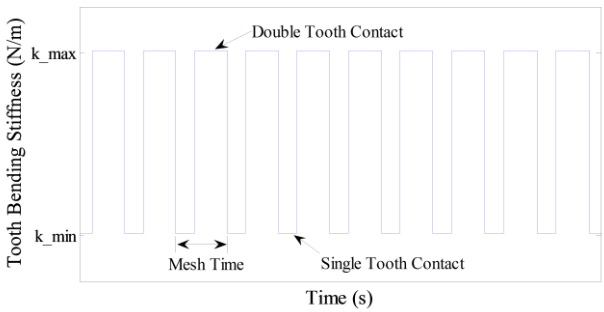

Figure 2. Variation in tooth bending stiffness during meshing of gears

In this paper, only rotational motions of gears are modeled without considering lateral motion, which will be considered in the future when the effect of bearings is modeled. A torque balance of the lumped masses representing the gearbox is carried out, such that the system is at equilibrium during its dynamic operation. This method generates the following set of coupled differential equations of motion which represents the dynamic operation of the gearbox.

$$\left(I_c + \frac{3m_p r_c^2}{\cos^2\alpha}\right)\ddot{\theta}_c - r_c k_{rp}(3r_s\theta_s - 6r_c\theta_c) - r_c q_{rp}(3r_s\dot{\theta}_s - 6r_c\dot{\theta}_c) = T_{in} \quad (1)$$

$$I_p\ddot{\theta}_p + r_p k_{rp}(2r_p\theta_p - r_s\theta_s) + r_p q_{rp}(2r_p\dot{\theta}_p - r_s\dot{\theta}_s) = 0 \quad (2)$$

$$I_s\ddot{\theta}_s + r_s k_{rp}(3r_s\theta_s - 3r_p\theta_p - 3r_c\theta_c) + r_s q_{sp}(3r_s\dot{\theta}_s - 3r_p\dot{\theta}_p - 3r_c\dot{\theta}_c) + k_{s2}(\theta_s - \theta_1) + q_{s2}(\dot{\theta}_s - \dot{\theta}_1) = 0 \quad (3)$$

$$I_1\ddot{\theta}_1 + r_1 k_{mb1}(r_1\theta_1 - r_{2a}\theta_2) + r_1 q_{mb1}(r_1\dot{\theta}_1 - r_{2a}\dot{\theta}_2) - k_{s2}(\theta_s - \theta_1) - q_{s2}(\dot{\theta}_s - \dot{\theta}_1) = 0 \quad (4)$$

$$I_2\ddot{\theta}_2 + r_{2b}k_{mb2}(r_{2b}\theta_2 - r_3\theta_3) + r_{2b}q_{mb2}(r_{2b}\dot{\theta}_2 - r_3\dot{\theta}_3) + r_{2a}k_{mb1}(r_{2a}\theta_2 - r_1\theta_1) + r_{2a}q_{mb1}(r_{2a}\dot{\theta}_2 - r_1\dot{\theta}_1) = 0 \quad (5)$$

$$I_3\ddot{\theta}_3 + r_3 k_{mb2}(r_3\theta_3 - r_{2b}\theta_2) + r_3 q_{mb2}(r_3\dot{\theta}_3 - r_{2b}\dot{\theta}_2) = T_{el} \quad (6)$$

where,

		Subscripts:	
I	inertia	s	sun gear
θ	angular rotation	s_2	coupling shaft
$\dot{\theta}$	angular velocity	p	planet
$\ddot{\theta}$	angular acceleration	c	Carrier
T	torque	rp	ring and planet
K	stiffness	i	number of the planet gear (1, 2 or 3)
Q	damping	mb	tooth bending
R	base circle radius	in	input
α	pressure angle of gear tooth	el	electrical

The system of differential equations is solved using the Runge-Kutta method–based solvers of Simulink® software from Mathworks, Inc. Finite element analysis of gear tooth profiles in mesh with a crack has been shown to exhibit a reduced tooth bending stiffness than that without a crack [9]. This concept is implemented in this model to simulate the operation of the gearbox with a crack in one of the gear teeth. The variation of tooth bending stiffness due to a crack in a gear tooth in the input gear carried out in this study is shown in Fig. 3.

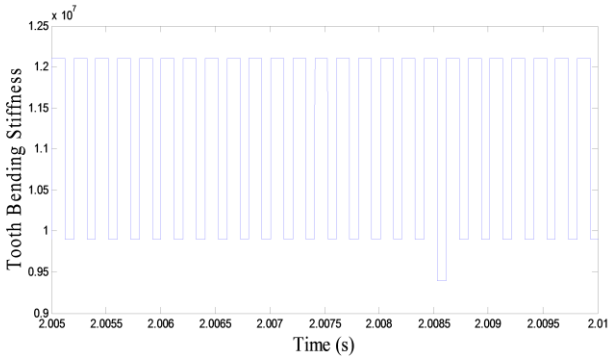

Figure 3. Variation in tooth bending stiffness due to crack in a gear tooth

B. *Dynamic modeling of a doubly fed induction generator*

The commonly used d-q reference frame model is used to model the time-varying inductances occurring due to the relative motion between the rotor and stator fluxes [15]. This model requires the transformation of the three phase voltages of the induction generator into the stationary d-phase and q-phase. Since the rotor and stator voltages are in constant relative motion, the stationary axis voltages are transformed into a synchronous rotating reference frame called the d-q axis which rotates at the frequency of the voltage in the grid.

Using Ohm's law and Faraday's law, the dynamic equations of the generator are given by the following equations.

$$\frac{d\varphi_{Sq}}{dt} = v_{Sq} - \omega_e \varphi_{Sq} + \frac{R_S}{\sigma L_S}\left(\frac{M}{L_r}\varphi_{rq} - \varphi_{Sq}\right) \quad (7)$$

$$\frac{d\varphi_{Sd}}{dt} = v_{Sd} + \omega_e \varphi_{Sd} + \frac{R_S}{\sigma L_S}\left(\frac{M}{L_r}\varphi_{rd} - \varphi_{Sd}\right) \quad (8)$$

$$\frac{d\varphi_{rq}}{dt} = v_{rq} - (\omega_e - \dot{\theta}_r)\varphi_{rd} + \frac{R_r}{\sigma L_r}\left(\frac{M}{L_S}\varphi_{Sq} - \varphi_{rq}\right) \quad (9)$$

$$\frac{d\varphi_{rd}}{dt} = v_{rd} + (\omega_e - \dot{\theta}_r)\varphi_{rq} + \frac{R_r}{\sigma L_r}\left(\frac{M}{L_S}\varphi_{Sd} - \varphi_{rd}\right) \quad (10)$$

The electrical torque generated in the rotor of the generator due to the rotation is given by

$$T_{el} = \frac{3pM}{4\sigma L_S L_r}\left(\varphi_{Sq}\varphi_{rd} - \varphi_{Sd}\varphi_{rq}\right) \quad (11)$$

where

$$\sigma = 1 - (M^2/L_R L_S) \quad (12)$$

In the above equations, subscripts s and r respectively represent the stator and rotor quantities, subscripts d and q represent quantities in the d-q reference frame, φ is the magnetic flux, R is the resistance, L is the self-inductance, M is the mutual inductance and ω_s is the angular velocity of the AC voltage. These equations are also modeled in Simulink and coupled with the mechanical equations of the gearbox.

C. *Simulation*

The simulation of the wind turbine is carried out based on the wind turbine parameters in reference [11]. The coupled mechanical and electrical equations are simulated for an input torque of 34654 Nm, which corresponds to a nominal operating condition. The corresponding output torque from the gearbox is 999.91 Nm. The equations are simulated for the steady state operation of the system. The corresponding initial condition of the system for the given input torque is shown in Table 1. These initial conditions are calculated from (1) - (6) by vanishing all acceleration terms.

TABLE I. INITIAL CONDITION FOR SIMULATION FOR INPUT TORQUE

Component	**Initial Angular velocity (rad/s)**
Carrier gear	11.0
Planet gear	18.6
Sun gear	54.0
Gear 1	54.0
Gear 2	164.8
Gear 3	381.2

III. RESULTS

The simulated signal of angular velocity of the input and output gears of the gearbox is shown in Fig. 4. It can be seen that the simulation converges to the steady state after about 0.2s of simulation. Fig. 5 shows the frequency spectrum of the angular acceleration signals with and without a crack in gear 3. It has been established in the literature that side bands around the gear mesh frequency are the components which are sensitive to cracks in a gear tooth [16]. The simulation results with a fault in the gear teeth do agree with this finding. Analysis of the electrical torque signal generated in the DFIG also indicates this parameter is sensitive to the occurrence of cracks in a gear tooth. Fig. 6 shows the frequency spectrum of the electrical torque signal in the DFIG with and without a crack in gear 2a. It can be seen from the plot that specific frequencies are excited due to faults in specific gears of the gearbox. Peaks at 52.5 Hz can be observed due to a crack in gear 2a, whereas these peaks occur at 60.5 Hz due to a crack in gear 3 as shown in Fig. 7. Simulation of the model under faults in multiple components also show the occurrence of these peaks in the frequency spectrum of the electrical torque signal as can be observed in Fig. 8. Therefore, by monitoring frequencies of peaks in electromagnetic torque signals, it is possible to identify the location of faults in the gearbox.

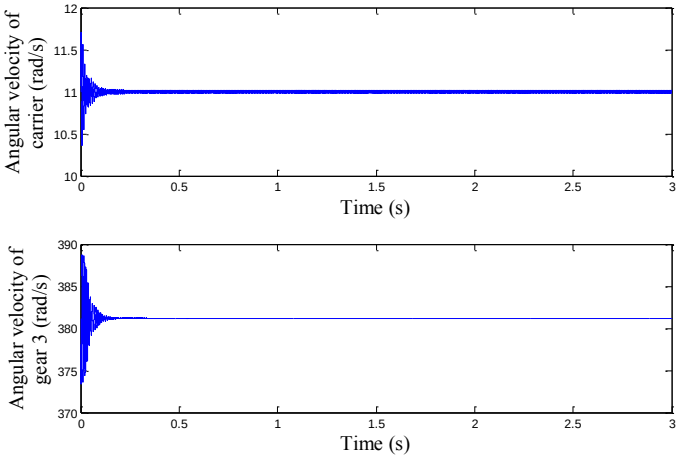

Figure 4. Simulation result of angular velocity during steady state operation

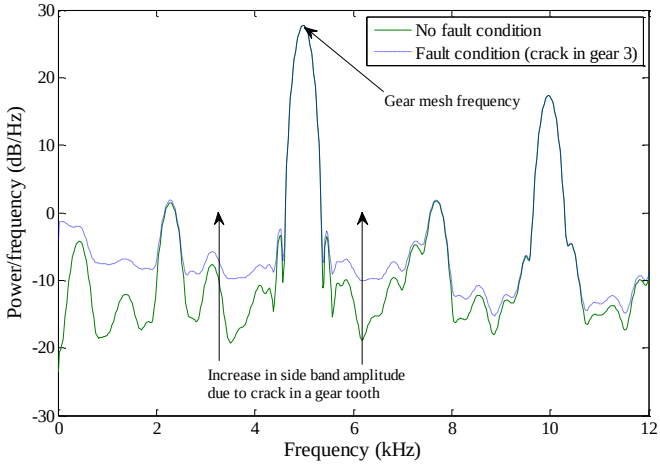

Figure 5. Comparison of frequency spectrum of angular acceleration of gear 3 with and without a crack in gear 3

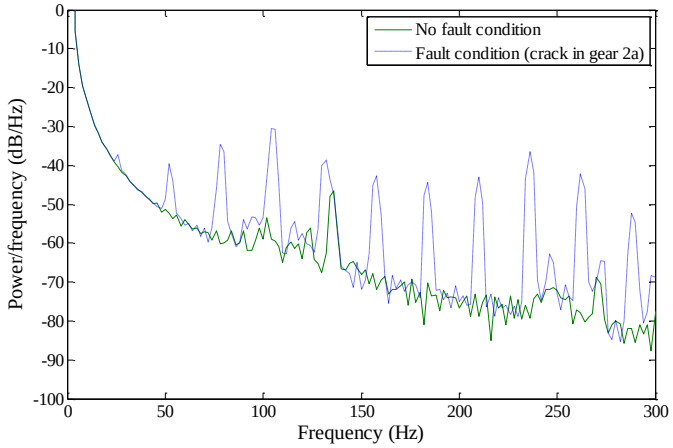

Figure 6. Comparison of frequency spectrum of electrical torque signal with and without a crack in gear 2a

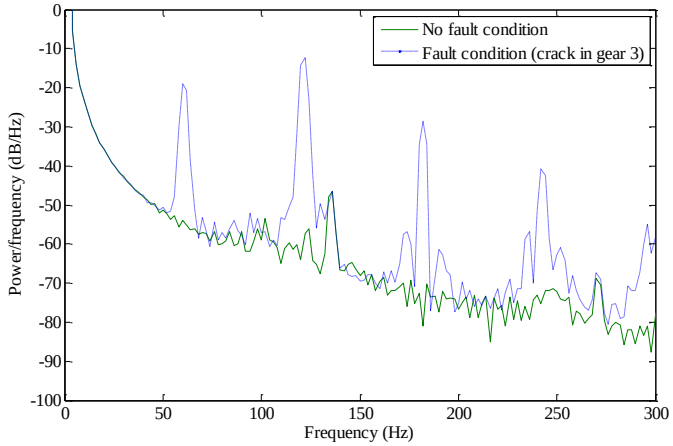

Figure 7. Comparison of frequency spectrum of electrical torque signal with and without a crack in gear 3

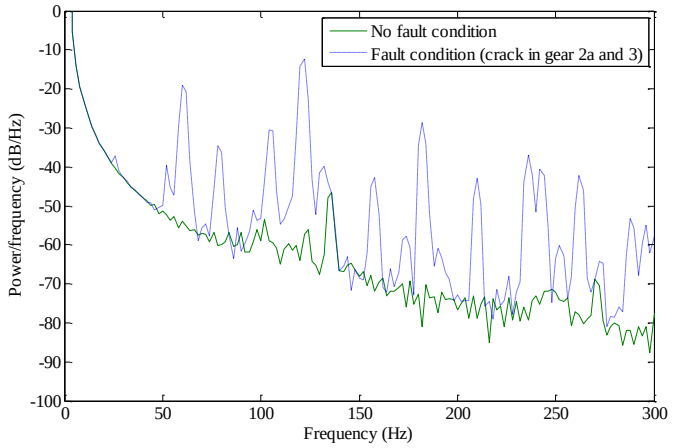

Figure 8. Comparison of frequency spectrum of electrical torque signal with and without a crack in gear 2a and 3

IV. CONCLUSIONS

A methodology for fault simulation using a coupled model of mechanical and electrical systems in a wind turbine is presented in this study. Simulation using the mechanical model has confirmed that a crack in a gear tooth can be detected using the angular acceleration of the gear. This analysis has shown that the crack in a gear tooth of a wind turbine can also be detected in the electrical torque signal of the wind turbine, which can be calculated from the electrical current output signal of the wind turbine. The important results from this study are summarized below:

1. Fault detection using mechanical signals often require knowledge about the healthy state of the mechanical components, whereas this knowledge is not required when analyzing the electrical torque signal since peaks corresponding to faults occur only when the faults are present in the mechanical components.

2. Identification of the exact faulty component in a complex system is often difficult using mechanical signals, since the fault's characteristic features could overlap for different components. Electrical torque signal analysis, however, shows that specific frequencies are excited due to the periodic nature of the fault in a specific component. Identification of these peaks in the frequency spectrum of the electrical torque signal can lead to the identification of the exact component in the system which has the fault.

3. Another advantage of using the electrical torque signals for fault detection is that the signals can be observed in low frequency ranges, rather than the analysis of the mechanical signals which require high frequency ranges for fault detection. This would reduce the demand on the data acquisition sensors, memory and processing hardware required for detection of faults.

Future work will involve the validation of the results using data from a real system, as well as the development of methodology for the detection of different faults such as rotor blade and bearing faults.

REFERENCES

[1] M. El Hachemi Benbouzid, "A review of induction motors signature analysis as a medium for faults detection," *Industrial Electronics, IEEE Transactions on*, vol. 47, no. 5, pp. 984–993, 2000.

[2] Wenxian Yang, P. J. Tavner, C. J. Crabtree, and M. Wilkinson, "Cost-Effective Condition Monitoring for Wind Turbines," *Industrial Electronics, IEEE Transactions on*, vol. 57, no. 1, pp. 263–271, 2010.

[3] S. J. Watson, B. J. Xiang, Wenxian Yang, P. J. Tavner, and C. J. Crabtree, "Condition Monitoring of the Power Output of Wind Turbine Generators Using Wavelets," *IEEE Transactions on Energy Conversion*, vol. 25, no. 3, pp. 715–721, Sep. 2010.

[4] C. J. Crabtree, S. Djurovic, P. J. Tavner, and A. C. Smith, "Condition monitoring of a wind turbine DFIG by current or power analysis," in *Power Electronics, Machines and Drives (PEMD 2010), 5th IET International Conference on*, 2010, pp. 1–6.

[5] R. C. Healey, "The measurement of transient electromagnetic torque in high-performance electrical drives," 1996, vol. 1996, pp. 226–229.

[6] P. Novak, T. Ekelund, I. Jovik, and B. Schmidtbauer, "Modeling and control of variable-speed wind-turbine drive-system dynamics," *IEEE Control Systems*, vol. 15, no. 4, pp. 28–38, Aug. 1995.

[7] V. Akhmatov, H. Knudsen, and A. H. Nielsen, "Advanced simulation of windmills in the electric power supply," *International Journal of Electrical Power & Energy Systems*, vol. 22, no. 6, pp. 421–434, Aug. 2000.

[8] J. Ekanayake, L. Holdsworth, and N. Jenkins, "Control of DFIG Wind Turbines," *Power Engineer*, vol. 17, no. 1, p. 28, Feb. 2003.

[9] J. G. Slootweg, H. Polinder, and W. L. Kling, "Dynamic modelling of a wind turbine with doubly fed induction generator," in *Power Engineering Society Summer Meeting, 2001. IEEE*, 2001, vol. 1, pp. 644–649 vol.1.

[10] B. Boukhezzar and H. Siguerdidjane, "Nonlinear control with wind estimation of a DFIG variable speed wind turbine for power capture

optimization," *Energy Conversion and Management*, vol. 50, no. 4, pp. 885–892, Apr. 2009.
[11] M. Todorov, I. Dobrev, and F. Massouh, "Analysis of torsional oscillation of the drive train in horizontal-axis wind turbine," in *Advanced Electromechanical Motion Systems & Electric Drives Joint Symposium, 2009. ELECTROMOTION 2009. 8th International Symposium on*, 2009, pp. 1–7.
[12] S. A. Papathanassiou and M. P. Papadopoulos, "Dynamic behavior of variable speed wind turbines under stochastic wind," *Energy Conversion, IEEE Transactions on*, vol. 14, no. 4, pp. 1617–1623, 1999.
[13] J. Wang and I. Howard, "The torsional stiffness of involute spur gears," *Proceedings of the Institution of Mechanical Engineers, Part C: Journal of Mechanical Engineering Science*, vol. 218, no. 1, pp. 131 –142, Jan. 2004.
[14] I. Howard, S. Jia, and J. Wang, "The dynamic modelling of a spur gear in mesh including friction and a crack," *Mechanical Systems and Signal Processing*, vol. 15, no. 5, pp. 831–853, Sep. 2001.
[15] B. K. Bose, *Modern power electronics and AC drives*. Prentice Hall PTR, 2002.
[16] S. Goldman, *Vibration spectrum analysis: a practical approach*. Industrial Press Inc., 1999.

Ranjith Kumar received his B.E. degree in mechanical engineering from the College of Engineering Guindy, Anna University, India. He is currently working toward the Ph.D. degree in mechanical engineering at the University of Maryland, College Park.

He is a Graduate Research Assistant with the Center for Advanced Life Cycle Engineering, University of Maryland. His research interests include reliability, dynamics, vibration, tribology and prognostics and health management.

Michael H. Azarian (M'99) received the B.S. degree in chemical engineering from Princeton University and the M.S. and Ph.D. degrees in materials science and engineering from Carnegie Mellon University.

He is a Research Scientist with the Center for Advanced Life Cycle Engineering (CALCE), University of Maryland, College Park. Prior to joining CALCE in 2004, he spent over 13 years in the data storage, advanced materials, and fiber optics industries. His research focuses on the analysis, detection, prediction, and prevention of failures in electronic products. He has advised many companies on reliability of electronic products, and is the author or co-author of numerous publications on solder joint degradation, electrochemical migration, capacitor reliability, electronic packaging, and tribology. He is the holder of five U.S. patents for inventions in data storage and contamination control.

Dr. Azarian was the Technical Editor of the recently published IEEE Standard 1624 on organizational reliability capability, for assessing suppliers of electronic products. He is currently leading the work group to revise IEEE Standard 1332, "Reliability Program for the Development and Production of Electronic Products." He is co-chair of the Miscellaneous Techniques subcommittee of the SAE G-19A standards committee on detection of counterfeit parts. He previously co-chaired iNEMI's Technology Working Group on Sensor Technology Roadmapping. He is on the Editorial Advisory Board of Soldering & Surface Mount Technology.

Michael G. Pecht (M'83–F'92) received the M.S. degree in electrical engineering and the M.S. and Ph.D. degrees in engineering mechanics from the University of Wisconsin, Madison.

He is the Founder of the Center for Advanced Life Cycle Engineering, University of Maryland, College Park, where he is also a George Dieter Chair Professor in mechanical engineering and a Professor in applied mathematics. He has been leading a research team in the area of prognostics for the past ten years and has now formed a new prognostics and health management consortium at the University of Maryland. He has consulted for over 100 major international electronics companies, providing expertise in strategic planning, design, test, prognostics, IP, and risk assessment of electronic products and systems. He is the Chief Editor for Microelectronics Reliability. He has written more than 20 books on electronic-product development and use and supply-chain management and over 400 technical articles.

Dr. Pecht is a Professional Engineer and a fellow of ASME and IMAPS. He served as the Chief Editor of the IEEE TRANSACTIONS ON RELIABILITY for eight years and on the Advisory Board of IEEE SPECTRUM. He is an Associate Editor for the IEEE TRANSACTIONS ON COMPONENTS AND PACKAGING TECHNOLOGY. He was the recipient of the highest reliability honor, the IEEE Reliability Society's Lifetime Achievement Award in 2008. He was also the recipient of the European Micro and Nano-Reliability Award for outstanding contributions to reliability research, the 3M Research Award for electronics packaging, and the IMAPS William D. Ashman Memorial Achievement Award for his contributions in electronics reliability analysis.

Nam H. Kim (M'99) received the B.S. degree in mechanical engineering from Seoul National University, Korea, M.S. degree in mechanical engineering in Korea Advanced Institute of Science and Technology, and Ph.D. degree in the University of Iowa.

He is the Associate Professor in the Department of Mechanical and Aerospace Engineering at the University of Florida, where he is also leading the Structural and Multidisciplinary Optimization group. His research area is design under uncertainty and optimization, structural health monitoring and prognostics, nonlinear structural mechanics, and structural-acoustics. He has published more than hundred refereed journal and conference papers in the above areas.

Dr. Kim is an associate fellow of AIAA. He served as an associate editor of Structural and Multidisciplinary optimization and International Journal of Reliability.